



Effects of fluorines on nonsecosteroidal vitamin D receptor agonists

Hirota Kashiwagi*, Masateru Ohta, Yoshiyuki Ono, Kenji Morikami, Susumu Itoh, Hideki Sato, Tadakatsu Takahashi

Research Division, Chugai Pharmaceutical Co. Ltd, 1-135 Komakado, Gotemba, Shizuoka 412-8513, Japan

ARTICLE INFO

Article history:

Received 29 October 2012

Revised 20 November 2012

Accepted 21 November 2012

Available online 2 December 2012

Keywords:

Vitamin D₃
VDR agonist
Nonsecosteroidal
Bisphenylmethane
Fluorine interaction

ABSTRACT

From our research of nonsecosteroidal vitamin D₃ derivatives with gamma hydroxy carboxylic acid, we identified compound **6**, with two CF₃ groups in the side chain, as a most potent vitamin D receptor (VDR) agonist that shows superagonistic activity in VDRE reporter gene assay, MG-63 osteocalcin production assay and HL-60 cell differentiation assay. Compound **6** demonstrated that fluorination is as effective in the case of our nonsecosteroidal scaffold as in the case of secosteroidal VD₃ analogs. X-ray analysis of the VDR with compound **6** revealed all of the six fluorine atoms of the hexafluoropropanol (HFP) moiety in the side chain effectively interacting with the VDR by both steric (van der Waals) and electrostatic (hydrogen bond, NH–F and CH–F) interactions. The HFP moiety of **6** effectively interacts with helix 12 (H12) of the VDR and stabilizes the position and the orientation of H12, which could result in stabilizing the coactivator and enhancing the VDR agonistic activity.

© 2012 Elsevier Ltd. All rights reserved.

1. Introduction

In the field of medicinal chemistry, introducing a fluorine atom is a very useful way of increasing activity and selectivity, blocking metabolic sites, and modifying physicochemical properties such as solubility and permeability.¹ Recently, structural information gained from database surveys and numerous published works provides information on various types of fluorine-related interactions, such as orbital interaction, closed-shell interaction, anti-parallel dipolar interaction, orthogonal multipolar interaction, and hydrogen bonding, to help rationalize the contribution of fluorine to protein binding.^{2–15}

In research on secosteroidal vitamin D₃ analogs, fluorine substitutions were attempted with a replacement of the hydrogen atoms on carbon atoms at 24, 26 and 27 positions in the side chain moiety,^{16–20} and a replacement of the hydroxy group at 1, 3 and 25 positions.^{21–23} From these many efforts, hexafluoro-substituted derivative of 1 α ,25-dihydroxyvitamin D₃ (1,25(OH)₂D₃, **1**), falecalcitriol (**2**) was discovered (Fig. 1). The structural feature of **2** was two trifluoromethyl (CF₃) groups at 26 and 27 positions in the side chain part of the secosteroidal scaffold. It exhibited very potent activity in vitro and also in vivo^{18,19} and was launched as an anti-hyperparathyroidism drug in 2001. Thus, fluorination of the side chain is an attractive modification in vitamin D₃ research.

In 1999, Boehm et al. reported the first nonsecosteroidal vitamin D₃, LG190178 (**3**) and since then various groups have reported

its derivatives.^{24–30} We have synthesized the bisphenyl core compounds with gamma hydroxy carboxylic acid moiety in the A-part, such as **4**, and found this class of compounds showed vitamin D₃ agonist activity. Through systematic modification of the side chain part, compound **4** with an (*E*)-olefin linker and terminal diethyl group in the side chain showed a potency equal to that of 1,25(OH)₂D₃ in vitro (Fig. 1).^{31,32}

After the discovery of **4**, we attempted to introduce a hexafluoropropanol (HFP) moiety into the side chain to increase vitamin D₃ receptor (VDR) agonistic activity further. Additionally, in order to examine in detail the interactions between VDR and a molecule with an HFP moiety, we determined the 3D structures of VDR in complex with compounds **5** and **6** by X-ray crystallography.

2. Chemistry

The synthesis of compounds **5–7** is shown in Scheme 1. Compound **8** was prepared by the method reported previously.³² Lithiation of **8** with *n*-butyllithium and consequent treatment of hexafluoroacetone gas gave acetylenealcohol **9** in 68% yield. This acetylene **9** was selectively reduced to (*E*)-olefin **11** by Red-Al® in 80% yield. Before O-alkylation of the phenol group, the acidic hydroxy groups in the side chain of **9** and **11** were protected by a methoxymethyl (MOM) group to avoid di-O-alkylation. The alkylation of phenol groups in **10** and **12** with (*S*)-(+)-dihydro-5-(*p*-tolylsulfonyloxymethyl)-2(3*H*)-furanone (**13**) in the presence of potassium carbonate at 100 °C afforded lactones **14** and **15** in good yields. The MOM groups of **14** and **15** were removed by concentrated hydrogen chloride with excellent yields (95% and 96%).

* Corresponding author.

E-mail address: kashiwagihrt@chugai-pharm.co.jp (H. Kashiwagi).

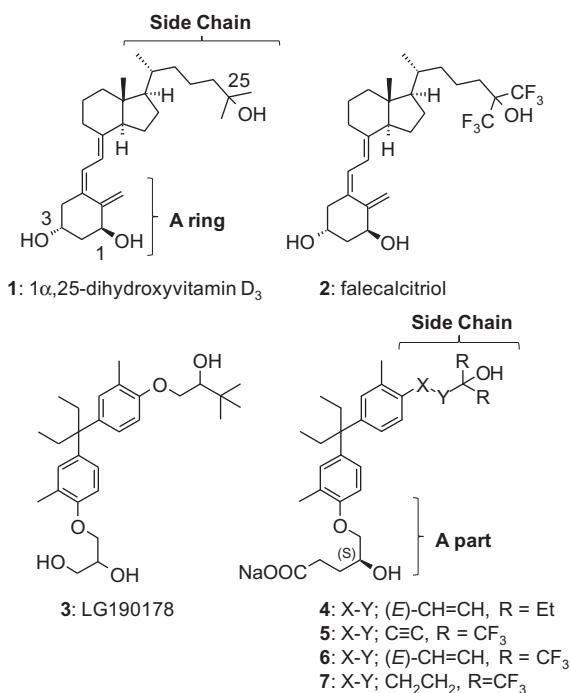


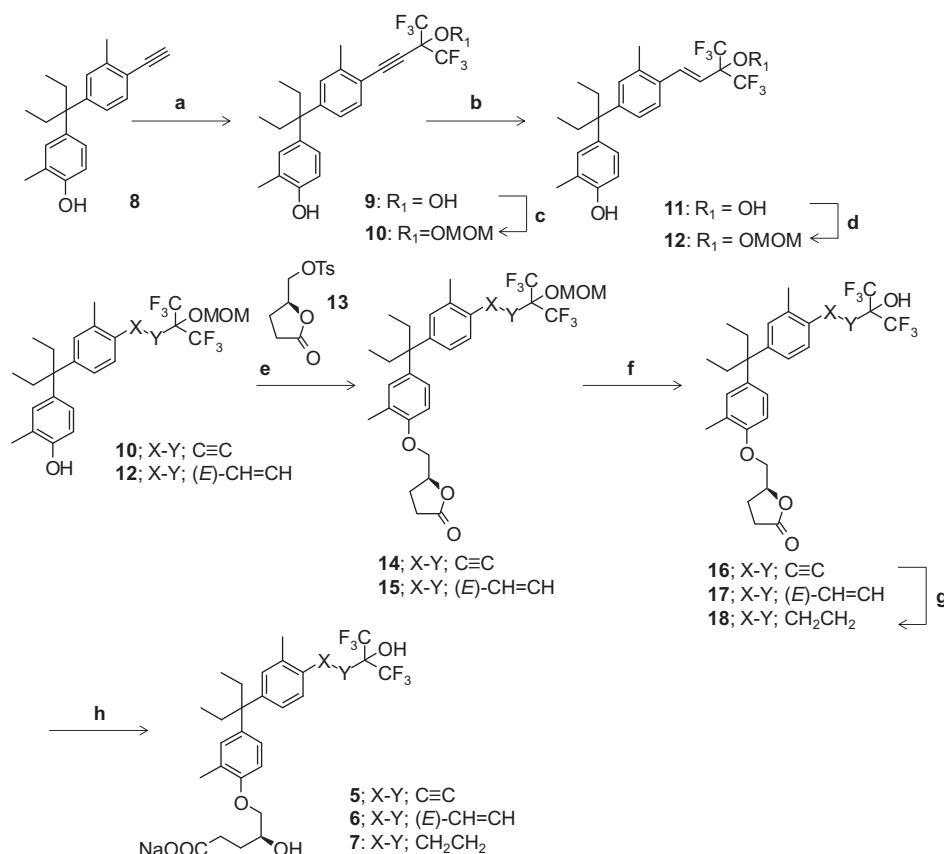
Figure 1. Structures of secosteroids 1 α ,25-dihydroxyvitamin D₃ (1), falecalcitriol (2), nonsecosteroidal analog LG190178 (3) and a series of nonsecosteroidal analogs with carboxylic acid (4–7). Part labeled A of 4–7 shows the structural correspondence to the A ring of secosteroids (upper left).

Methylene analog **18** was prepared with hydrogenation of acetylene alcohol **16** in the presence of a catalytic amount of palladium hydroxide in 95% yield. The lactones **16**, **17** and **18** were hydrolyzed to gamma hydroxy carboxylic acid free form by being treated with 1 M potassium hydroxide solution and then acidified with saturated ammonium chloride solution. These carboxylic acids were converted to sodium salts **5**, **6**, and **7** using 1.0 equiv amount of 1 M sodium hydroxide solution to avoid retro lactone formation during long time storage.

3. Results and discussion

In order to evaluate the VDR agonistic activity, the compounds synthesized were evaluated by three different assays. The first one is a reporter gene assay (RGA) in MG-63 cells which contains the VDRE sequence derived from mouse osteopontin promoter. Secondly, the osteocalcin production activity in MG-63 cells was evaluated to measure bone formation activity of functional vitamin D agonistic effect.^{33–35} Thirdly, cell differentiation activity in HL-60 cells was evaluated to measure the standard VDR agonistic effect. All types of activity are represented by an EC₅₀ value relative to the EC₅₀ value of 1,25(OH)₂D₃, which is assigned as 100% (a higher figure means stronger activity).

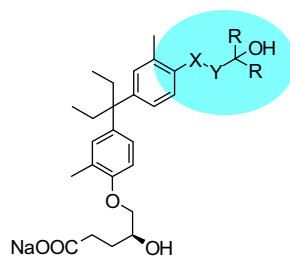
As expected, the HFP analogs with various linkers (**5**, **6** and **7**) exhibited very potent levels of activity (Table 1). In VDRE RGA, the acetylene linker analog **5** showed moderate activity (30%), and the methylene linker analog **7** showed activity comparable to 1,25(OH)₂D₃ but the (E)-olefin linker analog **6** showed sixfold stronger activity than that of 1,25(OH)₂D₃. In the HL-60 cell



Scheme 1. Reagents and conditions: (a) *n*-BuLi, hexafluoroacetone gas, 0 °C, THF, 68%; (b) Red-Al[®], 0 °C, THF, 80%; (c) K₂CO₃, MOMCl, room temp, DMF, 89%; (d) NaH, MOMCl, 50 °C, DMF, 41%; (e) K₂CO₃, **13**, 100 °C, DMF, 85–90%; (f) concd HCl, room temp, 1,4-dioxane, 95–96%; (g) Pd(OH)₂/C, H₂, room temp, MeOH, 95%; (h) (i) 1 M KOH, room temp, MeOH, (ii) satd NH₄Cl aq, (iii) 1 M NaOH, EtOH, 49–83%.

Table 1

In vitro activities and calculated side chain volumes and PCs



Compound	-X-Y-	R	Ratio of VDRE reporter gene ^a (%)	Ratio of HL-60 differentiation ^a (%)	Ratio of Osteocalcin ^a (%)	V _{side chain} ^b (Å ³)	PC ^c (%)
4	-(E)-CH=CH-	Et	105	126	447	117	56
5	-C≡C-	CF ₃	30	227	546	131	63
6	-(E)-CH=CH-	CF ₃	592	252	3746	132	64
7	-CH ₂ CH ₂ -	CF ₃	91	106	429	134	65
LG190178			6.7	71	185		
1,25(OH) ₂ D ₃			100	100	100		

^a 1,25(OH)₂D₃ ratio of EC₅₀. 1,25(OH)₂D₃ was assigned to 100% (higher figure means stronger activity).

^b Calculated volume of extracted side chain moiety from whole molecule (highlighted in blue on structure).

^c PC was calculated as follows: (V_{side chain}/208 Å³) × 100 (%).

differentiation assay, all of the HFP analogs were equally potent to or more potent than 1,25(OH)₂D₃: respectively, compounds **5** and **6** showed 2.2-fold and 2.5-fold the activity of 1,25(OH)₂D₃ and 1.8-fold and 2.0-fold the activity of compound **4**, which is the most active bisphenyl core compound with an alkyl side chain. In the osteocalcin assay, all of the HFP analogs showed stronger activity than 1,25(OH)₂D₃: respectively, compounds **5** and **7** showed 5.5-fold and 4.3-fold more potency than 1,25(OH)₂D₃, and the activity of **6** was a remarkable 37-fold. In most cases in the three assays, the HFP analogs showed activity equal to or more potent than 1,25(OH)₂D₃. The (E)-olefin linker analog **6** showed the most potent activity among the three HFP analogs and exhibited a super agonistic character in all of the three assays.

To confirm the detailed interactions between the HFP moiety and the VDR, we cocrystallized the ligand-binding domain of human VDR with compounds **5** and **6** in accordance with a method previously reported.³¹ The 3D structure of the VDRs in both complexes showed a typical nuclear hormone receptor fold consisting of 12 helices (Fig. 2A and B). The positions and the binding modes of **5** and **6** in the VDR were identical to those of non-fluorinated bisphenyl compounds.³¹ In spite of the linker difference, the positions of each atom (except the linker atoms) of **5** and **6** in the VDR were nearly identical and finely superimposed (Fig. 3A and B). In detail, the carboxyl group in the A-part of **5** and **6** had three key interactions: the salt bridge with Arg274 from helix 5 (H5) of the VDR, the hydrogen bond with the crystal water, and the intramolecular hydrogen bond with the gamma hydroxy group of the A part of **5** and **6** (Fig. 3A). The gamma hydroxy group of the A part made a hydrogen-bonding interaction also with the crystal water which made a hydrogen bond with the phenol oxygen of Tyr143 from helix 1 (H1). The phenyl group containing the A part was sandwiched between CH-π interactions with the Cβ of Ser275 (H5) and with the Cε of Leu233 from helix 3 (H3) (Fig. 3B). The bis-ethyl moiety between the phenyl rings made good CH-π interactions with the indole ring of Trp286 from the loop between H5 and helix 6 (H6). The phenyl group containing the side chains of **5** and **6** was also sandwiched between CH-π interactions with the Cγ of Val234 (H3) and with the Cγ of Val300 (H6).

Figure 4A shows the hydroxy group of the HFP moiety of **5** and **6** located at nearly identical positions, in spite of their linker differences. The hydroxy group of the HFP moiety had interactions with the NHs of the imidazole of His305 from the loop between H6 and

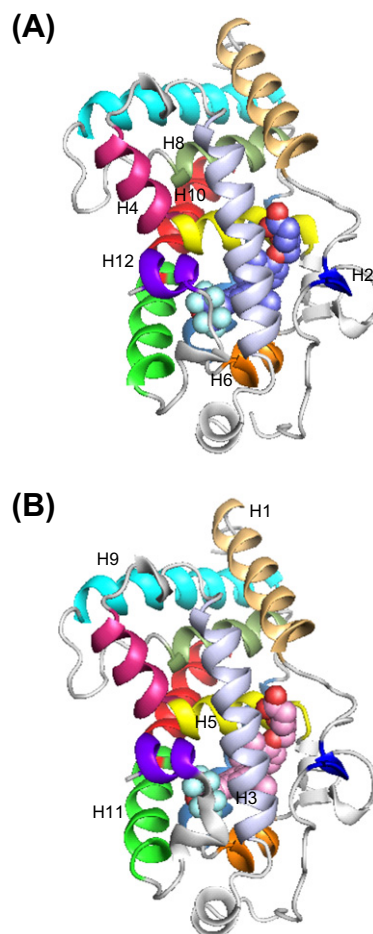


Figure 2. (A) X-ray crystal structure of VDR/compound **6** (slate) complex. (PDB ID: 3W0C) (B) X-ray crystal structure of VDR/compound **5** (pink) complex (PDB ID: 3W0A). Compounds **5** and **6** are represented by the spheres. VDRs are represented by their secondary structures. Different colors are assigned for each helix from 1 to 12.

helix 7 (H7) and His397 from helix 11 (H11) via a hydrogen bond, just as the 25-OH group of secosteroidal VD₃ analogs did (Fig. 4B).

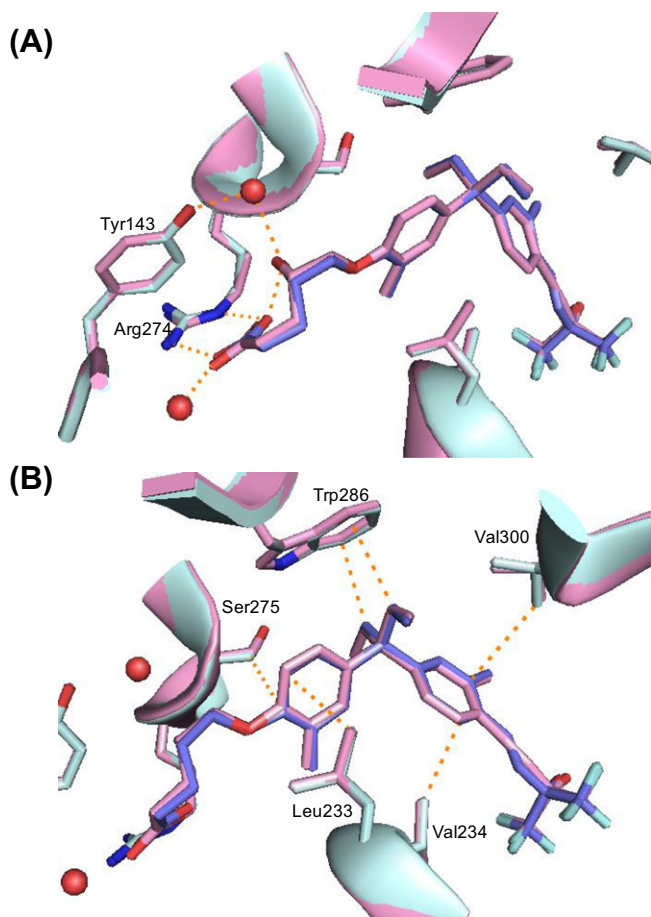


Figure 3. The superposition of the 3D structure of compound **5** (pink) and **6** (slate) in the VDR. The VDR complexed with **6** is colored in pale cyan and the VDR complexed with **5** is colored in pink. The crystallographic waters are depicted as red spheres. (A) The interactions between the A part of the ligand and the VDR. Hydrogen-bonding interactions are depicted by orange dashed lines. (B) The interactions between the bisphenyl core of the ligand and the VDR. CH- π interactions are depicted by orange dashed lines.

The distance of the hydrogen bond from the oxygen of the hydroxy group in the side chain of **5** to the imidazole nitrogen N ϵ of His397 was 2.7 Å, and that to the N ϵ of His305 was 2.9 Å. The distance from the hydroxy group of **6** to the N ϵ of His397 was 2.7 Å and that to the N ϵ of His305 was 2.7 Å. These short hydrogen bond distances indicated the strong hydrogen bond interaction of the hydroxy group of the HFP moiety. In the case of compounds **5**–**7**, the pK_a value of the hydroxy group of the HFP moiety was remarkably reduced because of the strong electron-withdrawing effect of two CF₃ groups. The calculated pK_a values of the hydroxy group of the HFP moiety by MoKa³⁶ are 6.7 for **5**, 8.5 for **6**, and 9.4 for **7**. These pK_a values are smaller than 17.1, which is the calculated pK_a value of the corresponding hydroxy group in the non-fluorinated compound **4**. This acidic pK_a is thought to contribute to the strong hydrogen bonding with two histidines of the VDR.

In addition to the hydrogen-bonding interactions of the hydroxy group of the HFP moiety, one of the fluorine atoms, F1, of the HFP moiety of **5** and **6** made an NH–F interaction with the imidazole nitrogen N ϵ of His397 (the distance between N ϵ and F1 was 3.3 Å for **5** and 3.1 Å for **6**) and the other fluorine atom, F6, also made an NH–F interaction with His305 (the distance between N ϵ and F6 was 3.2 Å for **5** and 3.4 Å for **6**) (Fig. 4B). In the case of an NH–F interaction, a positively-charged hydrogen (δ^+) attached to a nitrogen electrostatically interacts with a negatively charged fluorine (δ^-) favorably. These NH–F interactions further strengthen the attractive interaction between the HFP moiety and the VDR.

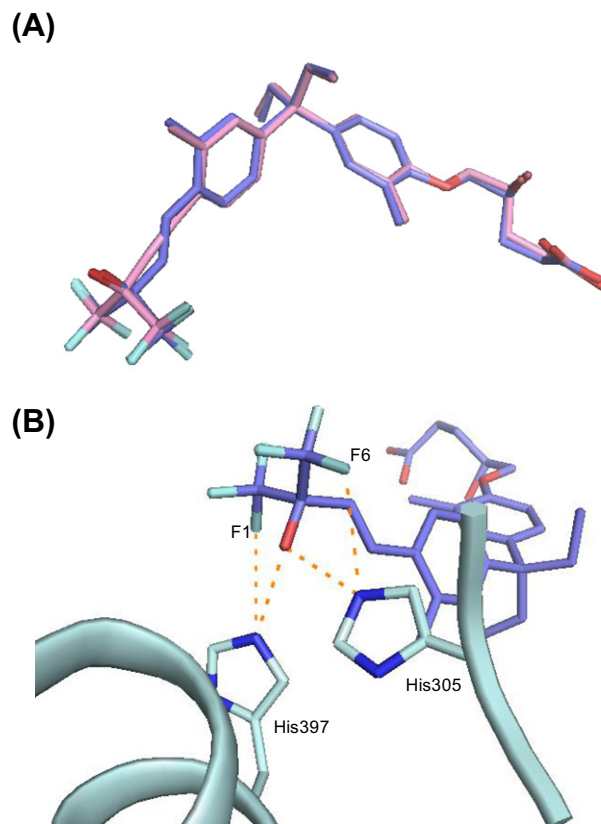


Figure 4. (A) The superposition of VDR bound conformation of compound **5** (pink) and **6** (slate) in each crystal. (B) The interactions between the HFP moiety of compound **6** (slate) and the VDR (pale cyan). Hydrogen bonds and NH–F interactions are depicted by orange dashed lines.

Two CF₃ groups of the HFP moiety of **5** and **6** were buried in the hydrophobic pocket formed by Leu227 (H3), Val234 (H3), Ile268 (H5), Tyr401 (H11), Leu414 from the loop between H11 and helix 12 (H12), and Val418 (H12), and Phe422 (H12) of the VDR (Fig. 5A). Furthermore, the two CF₃ groups were filling this hydrophobic pocket tightly. The atoms of the VDR located within 4 Å distance from the fluorine atoms of the HFP moiety are listed in Table 2. The number of contacts between fluorine atoms and the VDR atoms within 4 Å distance were 24 for **6** and 25 for **5**. These VDR atoms made good van der Waals (vdW) interactions with fluorine atoms and the tight vdW interactions increased the affinity of **5** and **6** with the VDR further.

Table 2 shows the detailed fluorine interactions around the side chain moiety of **5** and **6**. This detailed analysis revealed the existence of a large number of CH–F interactions around the HFP moiety (Fig. 5B). The hydrogen atom attached to one of the C δ atoms of Leu404 interacted with F1 and F2 and the C δ of Leu414 interacted with F1. With respect to Ala231, F3 interacted with the hydrogens attached to the C α and one of the C β atoms of Ala231. In the case of Val234, the hydrogens attached to all of the side chain carbons, C β and two C γ s, interacted with F4 and the hydrogen attached to one of the C γ atoms interacted also with F6. With regard to Val418, the hydrogen attached to one of the C γ atoms interacted with F5 and that on the other C γ interacted with F4. The hydrogens attached to one of the C δ and one of the C ϵ of Tyr401 interacted with F5 and the hydrogen attached to the C δ of Ile268 interacted with F6. In all of the CH–F interactions, a negatively-charged fluorine (δ^-) atom attractively interacts with a positively-charged (δ^+) hydrogen atom attached to carbon, although the δ^+ of the hydrogen is small. Thus, the large number of small and attractive electrostatic

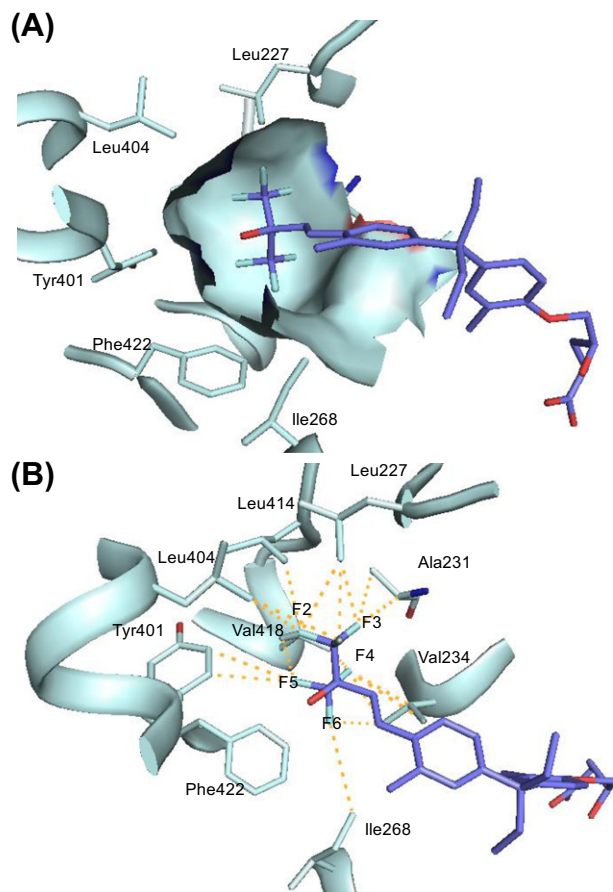


Figure 5. (A) Hydrophobic pocket of the VDR around the HFP moiety of **6**. Compound **6** is colored slate. VDR is colored in pale cyan. (B) CH–F interactions between the HFP moiety of **6** and the VDR. CH–F interactions are depicted by orange dashed lines.

Table 2

The list of fluorine atoms of compounds **6** and **5** and the residue atoms of the VDR within 4 Å distance of each other

6				5			
F	Residue	Atom	Distance (Å)	F	Residue	Atom	Distance (Å)
F1	Leu227	CD1	3.1	F1	Leu227	CD1	3.1
	His305	CD2	3.5		His305	CD2	3.7
	His305	NE2	3.2		His305	NE2	3.4
	Leu404	CD2	3.8		Leu404	CD2	3.8
F2	Leu227	CD1	3.4	F2	Leu227	CD1	3.4
	Leu404	CD2	3.5		Leu404	CD2	3.4
	Leu414	CD2	3.5		Leu414	CD2	3.4
F3	Leu227	CD1	3.1	F3	Leu227	CD1	3.3
	Ala231	CA	3.3		Ala231	CA	3.6
	Ala231	CB	3.5		Ala231	CB	3.8
	Ala231	N	3.4		Ala231	N	3.7
F4	Val234	CB	3.3	F4	Val234	CB	3.5
	Val234	CG1	3.4		Val234	CG1	3.4
	Val234	CG2	3.7		Val234	CG2	3.7
	Val418	CG2	3.8				
F5	Tyr401	CD1	3.5	F5	Tyr401	CD1	3.5
	Tyr401	CE1	3.7		Tyr401	CE1	3.6
	Val418	CG1	3.4		Val418	CG1	3.4
	Phe422	CD1	3.7		Phe422	CD1	3.6
					Phe422	CE1	3.9
F6	Val234	CG1	3.9	F6	Val234	CG1	3.6
	Ile268	CD1	3.9		Ile268	CD1	3.9
	His397	CE1	3.6		His397	CE1	3.5
	His397	NE2	3.3		His397	NE2	3.1
	Phe422	CE1	3.5		Phe422	CE1	3.4
					Phe422	CZ	3.8

interactions enhances further the favorable interaction between the HFP moiety and the VDR.

As described above, four factors are thought to be the cause of the favorable interactions between the HFP moiety and the VDR in view of the 3D structure. Firstly, the hydroxy group of the HFP moiety acidified by two electron-withdrawing CF₃ groups makes strong hydrogen bonds with two histidines of the VDR. Secondly, two NH–F interactions between two fluorine atoms and two histidines of the VDR increase favorable electrostatic interactions. Thirdly, two CF₃ groups fill the hydrophobic pocket of the VDR tightly and this results in a gain of vdW interaction energy between the HFP moiety and the VDR. Fourthly, a large number of weak but attractive CH–F interactions strengthen the favorable interaction between the HFP and the VDR.

We previously reported that there exists an optimal packing coefficient (PC) of around 55% in the hydrophobic pocket of the VDR occupied by the side chain of the ligand, and the PC of the side chain of compound **4** was very close to the ideal PC.³² In order to check whether the 55% rule can also be applied to HFP analogs, the PC values of **5**, **6** and **7** were calculated in the manner we reported previously.³² The calculated PC values were 63% for **5**, 64% for **6**, and 65% for **7**. It is apparent that the PC values of these fluorinated analogs were larger than the optimal value (55%) and the SAR of the fluorinated analogs could not be explained by the PC effect. The 55% rule is originally a rule that was derived from the case where a hydrophobic guest molecule binds to a hydrophobic pocket of the host molecule. Thus, the interactions involved in the 55% rule are mainly hydrophobic interactions. But, in the case of the interaction between a molecule with a HFP moiety and the VDR, electrostatic interactions such as hydrogen bonds, NH–F, and CH–F are included, as described above. These electrostatic interactions induced by the HFP moiety seem to be a reason for the discrepancy between the 55% rule and the SAR of compounds with a HFP moiety.

Regarding the activation of nuclear hormone receptors (NHR), it is known that H12 of the NHR interacts with their coactivator and plays a key role in exhibiting agonistic activity. 3D structures of NHR/coactivator/agonist complex revealed that the side chain of Glu from H12 of NHR makes hydrogen bonds with the main chain NHs of the coactivator peptides and these hydrogen bonds contribute to recruit the coactivator.³⁷ Three secosteroidal VD₃ analogs (Fig. 6) with the HFP moiety in the side chain were reported and all of them showed super agonistic activity.^{38,39} The 3D structures of zebra fish (z)VDR in complex with the coactivator SRC-1 peptide with a LXXLL-motif, and these three secosteroidal VD₃ analogs, CD578 (PDB ID: 3DR1),³⁸ Gemini 0072 (PDB ID: 3O1E),³⁹ and Gemini 0097 (PDB ID: 3O1D),³⁹ were also reported. Figure 7A and B show the superposition of the three secosteroidal VD₃ analogs and two nonsecosteroidal analogs, **5** and **6**. The positions and the interactions of the HFP moiety of these five molecules are almost the same (Fig. 8A and B). The HFP moiety of both **5** and **6** interacts with Val418 and Phe422 from H12 and Leu414 from the loop between H11 and H12. These interactions stabilize the position of H12. In the case of the three secosteroidal analogs, the HFP moiety also interacts with Val444 and Phe448 from H12 of zVDR and Leu440 from the loop between H11 and H12, which are, respectively, the residues corresponding to Val418, Phe422 and Leu414 of human VDR, and these interactions stabilize the H12 and also stabilize the coactivator peptide via the interaction between Glu446 from H12 of zVDR and the coactivator peptide. Figure 8A and B show the superposition of the side chains of Val, Phe, Leu and Glu and the main chain traces of the 3D structures of these five VDR complexes. The positions and the orientation of the side chains of Val, Phe, Leu and Glu and the interactions between the Val, Phe and Leu residues and the HFP moiety are almost identical. These commonalities of the position of H12 and of the interactions

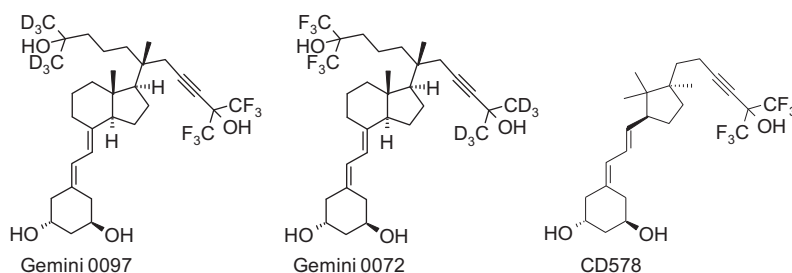


Figure 6. Fluorinated secosteroidal VD_3 analogs.

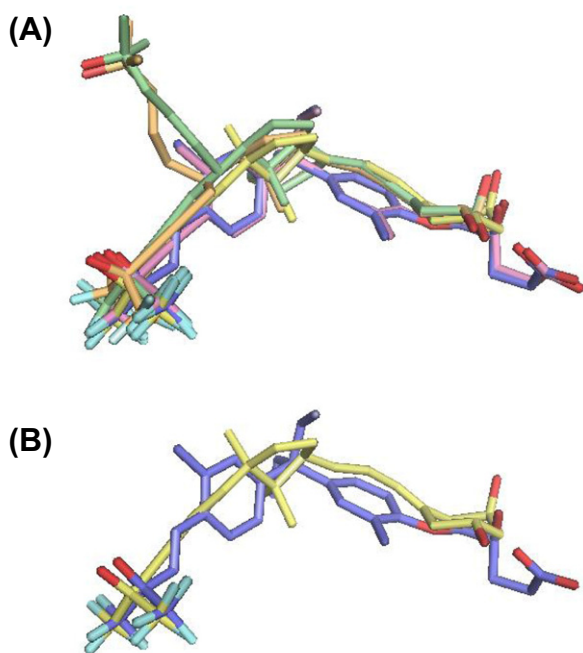


Figure 7. (A) The superposition of nonsecosteroidal VD_3 analogs, CD578 (pale yellow, PDB ID: 3DR1), Gemini 0097 (pale green, PDB ID: 3O1D), Gemini 0072 (light orange, PDB ID: 3O1E), and nonsecosteroidal analogs, **6** (slate) and **5** (pink) in the VDR. (B) The superposition of CD578 (pale yellow) and compound **6** (slate).

between H12 and the HFP moiety are assumed to be the reason for the superagonistic character exhibited by **5** and **6**.

Regarding the difference between the activity between acetylene linker **5** and (*E*)-olefin linker **6**, we could not explain the difference in the activity from their 3D information alone because the binding conformations of **5** and **6** were superposed well when bound to the VDR. Two factors to explain this difference are possible, just as in the case of the increase in activity of compound **4** (with ethyl groups at the terminal of the side chain) compared to that of the corresponding compound with an acetylene linker.³² The first possible reason is the hydrophobicity of the molecule. The $ClogP^{40}$ value of acetylene **5** is 6.13 and that of (*E*)-olefin **6** is 6.78. Thus, **6** is more hydrophobic than **5** and this could be the reason for the stronger activity of **6**. The second reason could be a loss of entropy from the bond rotation of the side chain. The rotation around a triple bond was reported to be almost free,⁴¹ but the rotation of the double bond in the olefin linker of **6** is restricted. When **5**, which has a triple bond, binds to the VDR and the bond rotation becomes fixed, there is a larger loss of entropy than when **6**, with a double bond, binds to the VDR. Therefore the larger loss of entropy of **5** compared to **6** could decrease the activity of **5**. It should be noted that, as described above, the pK_a value of **5** is more

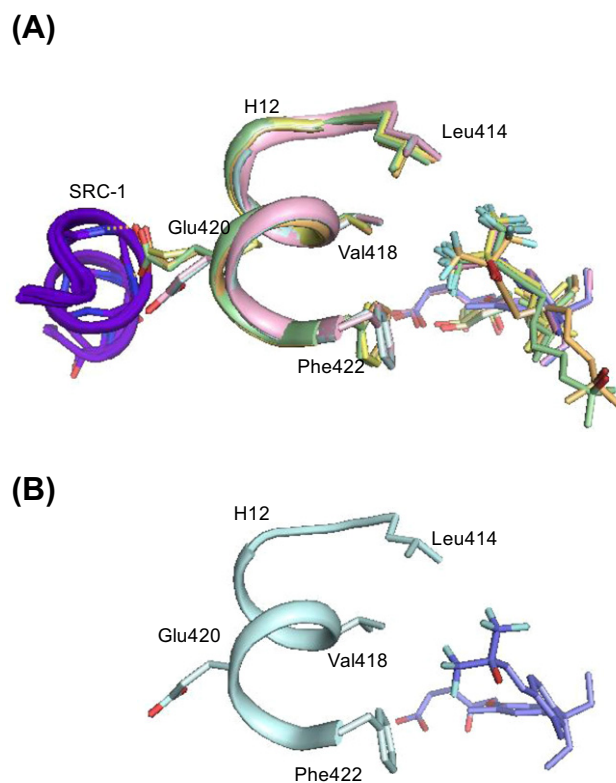


Figure 8. (A) The interactions between the HFP moiety of CD578 (pale yellow), Gemini 0097 (pale green), Gemini 0072 (light orange), compound **5** (pink), compound **6** (slate), the H12 of VDR, and SRC-1 coactivator peptide (purple/blue). The VDRs, other than the one in complex with **6**, are colored the same as their ligand. The VDR complexed with **6** is colored in pale cyan. The species of the VDRs in complex with CD578, Gemini 0097 and Gemini 0072 are zebra fish. SRC-1 coactivator peptide binds to zebra fish VDR (zVDR). The residue numbers depicted are those of human VDR (hVDR). The hydrogen bonds between Glu446 (Glu420 in hVDR number) and SRC-1 peptide are depicted by orange dashed lines. (B) The interactions between the H12 of hVDR and compound **6**. Compound **6** is colored in slate. The H12 of hVDR is colored in pale cyan.

acidic than that of **6**. Thus, the favorable electrostatic interaction energy of the hydroxy group of **5** with two histidines is thought to be larger than that of **6**. It is thought that the free energy gain of **6** by the two factors, hydrophobicity and entropy loss of the rotatable bond, is larger than the loss of electrostatic interaction energy caused by having a less acidic hydroxy group.

4. Conclusion

From our research of nonsecosteroidal vitamin D_3 derivatives with gamma hydroxy carboxylic acid, we identified compound **6**, which has two CF_3 groups in the side chain, as a most potent VDR agonist showing superagonistic activity in VDRE RGA, MG-63 osteocalcin production assay and HL-60 cell differentiation

assay. Compound **6** demonstrated that fluorination is effective in the case of our nonsecosteroidal scaffold, as it is in the case of secosteroidal VD₃ analogs. X-ray analysis of the VDR with compound **6** revealed that all of the six fluorine atoms of the HFP moiety in the side chain effectively interact with the VDR by both steric (vdW) and electrostatic (hydrogen bond, NH–F and CH–F) interactions. The HFP moiety of **6** effectively interacts especially with H12 of the VDR and stabilizes the position and the orientation of H12, which could result in stabilizing the coactivator and enhancing the VDR agonistic activity.

5. Experimental

5.1. Chemistry: general

Purchased reagents and solvents were used without further purification unless otherwise noted. ¹H and ¹³C NMR spectra were carried out on VARIAN 400-MR spectrophotometers; chemical shifts are reported in parts per million (ppm) downfield from that of internal tetramethylsilane (TMS). Mass spectrophotometry was measured with a Waters ACQUITY SQD electrospray ionization (ESI) system. High-resolution mass spectra (HRMS) were recorded on Thermo Fisher Scientific LTQ Orbitrap XL (ESI) instruments. Optical rotations were measured on a HORIBA SEPA-200 polarimeter (sodium D line at 25 °C). Chromatographic purification was carried out using Merck silica gel 60 (column) or Merck silica gel 60 PF₂₅₄ (preparative TLC).

5.1.1. 4-[1-Ethyl-1-[3-methyl-4-(4,4,4-trifluoro-3-hydroxy-3-trifluoromethyl-1-butyryl)phenyl]propyl]-2-methylphenol (**9**)

To a solution of **8** (16.44 g, 56.22 mmol) in THF (250 mL) was added *n*-butyllithium (2.71 M in *n*-hexane, 51.9 mL, 140.55 mmol) at 0 °C and the mixture was stirred for 30 min. To the mixture was added hexafluoroacetone by bubbling and the mixture was stirred at 0 °C for 30 min. Then the mixture was poured into satd NH₄Cl aq solution and products were extracted with AcOEt. The extracts were dried over anhydrous MgSO₄ and concentrated. The obtained residue was chromatographed on silica gel (*n*-hexane/AcOEt = 10:1 to 4:1) to afford **9** (17.62 g, 68%) as a colorless oil. ¹H NMR (CDCl₃) δ: 0.59 (6H, t, *J* = 7.3 Hz), 2.04 (4H, q, *J* = 7.3 Hz), 2.19 (3H, s), 2.38 (3H, s), 4.71 (1H, br s), 6.66 (1H, d, *J* = 8.0 Hz), 6.82–6.86 (2H, m), 6.99 (1H, d, *J* = 8.0 Hz), 7.05 (1H, s), 7.34 (1H, d, *J* = 8.2 Hz). ¹³C NMR (CDCl₃) δ: 152.2, 151.5, 140.8, 140.1, 131.8, 130.6, 129.4, 126.6, 125.7, 122.8, 122.6, 119.7, 116.2, 114.2, 89.5, 80.0, 49.3, 28.9, 20.6, 16.0, 8.3. MS (ESI negative): 457 (M–H)[–].

5.1.2. 4-[1-Ethyl-1-[3-methyl-4-(4,4,4-trifluoro-3-methoxymethoxy-3-trifluoromethyl-1-butyryl)phenyl]propyl]-2-methylphenol (**10**)

To a solution of **9** (356 mg, 0.777 mmol) in DMF (5 mL) was added K₂CO₃ (268 mg, 1.94 mmol) and the mixture was stirred for 20 min. To the mixture was added methoxymethyl chloride (0.071 mL, 0.935 mmol) and the mixture was stirred for 1 h. Then the mixture was poured into satd NH₄Cl aq solution and products were extracted with AcOEt. The extracts were washed with H₂O and brine, dried over anhydrous MgSO₄, and concentrated. The obtained residue was chromatographed on silica gel (*n*-hexane/AcOEt = 6:1) to afford **10** (349 mg, 89%) as a colorless oil. ¹H NMR (CDCl₃) δ: 0.59 (6H, t, *J* = 7.3 Hz), 2.04 (4H, q, *J* = 7.3 Hz), 2.19 (3H, s), 2.39 (3H, s), 3.48 (3H, s), 4.57 (1H, s), 5.15 (2H, s), 6.66 (1H, d, *J* = 8.8 Hz), 6.82–6.85 (2H, m), 6.99 (1H, dd, *J* = 8.1, 1.9 Hz), 7.05 (1H, d, *J* = 1.6 Hz), 7.37 (1H, d, *J* = 8.2 Hz). ¹³C NMR (CDCl₃) δ: 152.3, 151.9, 140.8, 139.7, 132.0, 130.5, 129.4, 126.4, 125.7, 123.1, 122.6, 119.7, 116.3, 114.1, 95.0, 93.3, 76.4, 56.4, 49.2, 28.9, 20.5, 16.1, 8.2. MS (ESI negative): 501 (M–H)[–].

5.1.3. 4-[1-Ethyl-1-[3-methyl-4-((E)-4,4,4-trifluoro-3-hydroxy-3-trifluoromethyl-1-butenyl)phenyl]propyl]-2-methylphenol (**11**)

To a solution of **9** (8.67 g, 18.91 mmol) in THF (100 mL) was added Red-Al[®] (65 wt% in toluene, 17 mL, 56.74 mmol) at 0 °C and the mixture was stirred for 1 h. The mixture was poured into 1 N HCl and products were extracted with CH₂Cl₂. The extracts were dried over anhydrous MgSO₄ and concentrated. The obtained residue was purified with silicagel chromatography (*n*-hexane/AcOEt = 10:1 to 4:1) to afford **11** (6.11 g, 70%) as a colorless oil. ¹H NMR (CDCl₃) δ: 0.61 (6H, t, *J* = 7.3 Hz), 2.05 (4H, q, *J* = 7.4 Hz), 2.19 (3H, s), 2.34 (3H, s), 4.59 (1H, br s), 6.08 (1H, d, *J* = 15.8 Hz), 6.66 (1H, d, *J* = 8.2 Hz), 6.85 (1H, dd, *J* = 8.4, 2.3 Hz), 6.88 (1H, d, *J* = 2.2 Hz), 7.00–7.02 (2H, m), 7.34 (1H, d, *J* = 7.6 Hz), 7.37 (1H, d, *J* = 15.7 Hz). ¹³C NMR (CDCl₃) δ: 151.5, 150.4, 140.4, 135.5, 135.1, 130.7, 130.5, 130.2, 126.5, 126.1, 125.3, 123.9, 122.8, 121.0, 116.4, 114.1, 49.0, 29.0, 19.9, 16.1, 8.3. MS (ESI negative): 459 (M–H)[–].

5.1.4. 4-[1-Ethyl-1-[3-methyl-4-((E)-4,4,4-trifluoro-3-methoxymethoxy-3-trifluoromethyl-1-butenyl)phenyl]propyl]-2-methylphenol (**12**)

To a solution of **11** (400 mg, 0.869 mmol) in DMF (5 mL) was added NaH (60% in mineral oil, 34.7 mg, 0.869 mmol) and the mixture was stirred for 30 min. To the mixture was added methoxymethyl chloride (0.132 mL, 1.74 mmol) and the mixture was stirred at 50 °C overnight. Then the mixture was poured into satd NH₄Cl aq solution and products were extracted with Et₂O. The extracts were washed with H₂O and brine, dried over anhydrous Na₂SO₄, and concentrated. The obtained residue was chromatographed on silica gel (*n*-hexane/AcOEt/CH₂Cl₂ = 10:1:1) to afford **12** (180 mg, 41%) as a colorless oil. ¹H NMR (CDCl₃) δ: 0.61 (6H, t, *J* = 7.3 Hz), 2.05 (4H, q, *J* = 7.4 Hz), 2.20 (3H, s), 2.32 (3H, s), 3.50 (3H, s), 4.60 (1H, br s), 4.97 (2H, s), 6.07 (1H, d, *J* = 16.6 Hz), 6.66 (1H, d, *J* = 8.2 Hz), 6.85 (1H, dd, *J* = 8.3, 2.2 Hz), 6.88 (1H, d, *J* = 2.2 Hz), 7.00–7.03 (2H, m), 7.34 (1H, d, *J* = 17.4 Hz), 7.35 (1H, d, *J* = 7.8 Hz). ¹³C NMR (CDCl₃) δ: 151.5, 150.6, 140.4, 137.7, 135.6, 131.1, 130.6, 130.2, 126.6, 126.3, 125.2, 123.8, 122.6, 121.0, 114.7, 114.1, 93.3, 56.4, 49.0, 29.0, 19.9, 16.1, 8.4. MS (ESI negative): 503 (M–H)[–].

5.1.5. General procedure for alkylation of the phenol group of **10** and **12**

To a solution of phenol (0.394 mmol) in DMF (4 mL) was added K₂CO₃ (0.985 mmol) and the mixture was stirred at room temperature for 30 min. Then, (*S*)-(+)-dihydro-5-(*p*-tolylsulfonyloxymethyl)-2(3*H*)-furanone (**13**) (0.591 mmol) was added and the mixture was stirred at 100 °C for 15 h. The mixture was poured into satd NH₄Cl aq solution and products were extracted with AcOEt. The extracts were washed with H₂O and brine, dried over anhydrous Na₂SO₄, and concentrated. The obtained residue was chromatographed on silica gel (*n*-hexane/AcOEt = 5:1 to 3:1) to afford lactone.

5.1.6. (*S*)-5-(4-[1-Ethyl-1-[3-methyl-4-(4,4,4-trifluoro-3-methoxymethoxy-3-trifluoromethyl-1-butyryl)phenyl]propyl]-2-methylphenoxy)methyl)dihydrofuran-2-one (**14**)

The yield was 85%. Colorless oil. [α _D²⁵]_D +9.58 (*c* 1.36, CHCl₃). ¹H NMR (CDCl₃) δ: 0.59 (6H, t, *J* = 7.2 Hz), 2.05 (4H, q, *J* = 7.3 Hz), 2.15 (3H, s), 2.27–2.36 (1H, m), 2.39 (3H, s), 2.41–2.49 (1H, m), 2.53–2.61 (1H, m), 2.72–2.81 (1H, m), 3.47 (3H, s), 4.07 (1H, dd, *J* = 10.3, 3.4 Hz), 4.17 (1H, dd, *J* = 10.4, 3.3 Hz), 4.86–4.91 (1H, m), 5.15 (2H, s), 6.67 (1H, d, *J* = 8.4 Hz), 6.86 (1H, d, *J* = 2.0 Hz), 6.92 (1H, dd, *J* = 8.5, 2.4 Hz), 6.98 (1H, dd, *J* = 8.0, 1.4 Hz), 7.04 (1H, s), 7.37 (1H, d, *J* = 8.0 Hz). ¹³C NMR (CDCl₃) δ: 177.1, 154.2, 152.0, 140.9, 140.5, 132.0, 130.6, 129.4, 126.1, 125.9, 125.6, 122.6,

119.7, 116.4, 110.0, 95.0, 93.2, 77.8, 77.2, 76.5, 69.4, 56.5, 49.3, 28.9, 28.3, 24.1, 20.6, 16.6, 8.3. MS (ESI positive): 618 (M+NH₄)⁺.

5.1.7. (S)-5-(4-{1-Ethyl-1-[3-methyl-4-((E)-4,4,4-trifluoro-3-methoxymethoxy-3-trifluoromethyl-1-butenyl)phenyl]propyl}-2-methylphenoxy)methyl) dihydrofuran-2-one (15)

The yield was 90%. Colorless oil. ¹H NMR (CDCl₃) δ: 0.61 (6H, t, *J* = 7.2 Hz), 2.06 (4H, q, *J* = 7.3 Hz), 2.16 (3H, s), 2.25–2.39 (1H, m), 2.32 (3H, s), 2.39–2.50 (1H, m), 2.53–2.61 (1H, m), 2.72–2.82 (1H, m), 3.50 (3H, s), 4.07 (1H, dd, *J* = 10.4, 3.5 Hz), 4.17 (1H, dd, *J* = 10.2, 3.3 Hz), 4.86–4.91 (1H, m), 4.96 (2H, s), 6.07 (1H, d, *J* = 16.6 Hz), 6.67 (1H, d, *J* = 8.4 Hz), 6.90 (1H, d, *J* = 2.0 Hz), 6.94 (1H, dd, *J* = 8.4, 2.2 Hz), 6.99 (1H, s), 7.00 (1H, d, *J* = 8.4 Hz), 7.34 (1H, d, *J* = 17.2 Hz), 7.35 (1H, d, *J* = 7.8 Hz). ¹³C NMR (CDCl₃) δ: 177.1, 154.1, 150.5, 140.9, 137.7, 135.6, 131.1, 130.6, 130.2, 126.2, 126.2, 125.8, 125.2, 123.8, 121.0, 114.7, 110.0, 93.3, 77.9, 77.2, 69.3, 56.4, 49.0, 29.0, 28.3, 24.1, 19.9, 16.6, 8.4. MS (ESI positive): 620 (M+NH₄)⁺.

5.1.8. (S)-5-(4-{1-Ethyl-1-[3-methyl-4-(4,4,4-trifluoro-3-hydroxy-3-trifluoromethyl-1-butynyl)phenyl]propyl}-2-methylphenoxy)methyl) dihydrofuran-2-one (16)

To a solution of **14** (19.5 mg, 0.032 mmol) in 1,4-dioxane (3.0 mL) was added concd HCl and the mixture was stirred at room temperature overnight. The mixture was poured into H₂O and products were extracted with CH₂Cl₂. The extracts were dried over anhydrous MgSO₄ and concentrated. The obtained residue was purified by preparative TLC (*n*-hexane/AcOEt = 2:1) to afford **16** (17.1 mg, 96%) as a colorless oil. [α_D^{25}] +11.1 (*c* 0.78, CHCl₃). ¹H NMR (CDCl₃) δ: 0.59 (6H, t, *J* = 7.3 Hz), 2.04 (4H, q, *J* = 7.2 Hz), 2.13 (3H, s), 2.25–2.35 (1H, m), 2.37 (3H, s), 2.40–2.48 (1H, m), 2.53–2.61 (1H, m), 2.73–2.82 (1H, m), 4.02–4.07 (1H, m), 4.13–4.17 (1H, m), 4.85–4.90 (1H, m), 6.65 (1H, d, *J* = 8.4 Hz), 6.85 (1H, d, *J* = 2.2 Hz), 6.91 (1H, dd, *J* = 8.5, 2.1 Hz), 6.97 (1H, d, *J* = 8.0 Hz), 7.03 (1H, s), 7.34 (1H, d, *J* = 8.2 Hz). ¹³C NMR (CDCl₃) δ: 177.6, 154.1, 151.9, 140.8, 140.6, 131.8, 130.6, 129.4, 126.1, 125.9, 125.7, 122.6, 119.8, 116.4, 110.0, 89.3, 80.1, 78.0, 77.2, 69.3, 49.3, 28.9, 28.4, 24.0, 20.5, 16.6, 8.3. MS (ESI positive): 579 (M+Na)⁺.

5.1.9. (S)-5-(4-{1-Ethyl-1-[3-methyl-4-((E)-4,4,4-trifluoro-3-hydroxy-3-trifluoromethyl-1-butenyl)phenyl]propyl}-2-methylphenoxy)methyl) dihydrofuran-2-one (17)

The yield was 95%. Colorless oil. [α_D^{25}] +11.1 (*c* 0.71, CHCl₃). ¹H NMR (CDCl₃) δ: 0.60 (6H, t, *J* = 7.2 Hz), 2.05 (4H, q, *J* = 7.2 Hz), 2.15 (3H, s), 2.27–2.35 (1H, m), 2.33 (3H, s), 2.39–2.48 (1H, m), 2.52–2.61 (1H, m), 2.73–2.81 (1H, m), 4.06 (1H, dd, *J* = 10.3, 3.4 Hz), 4.16 (1H, dd, *J* = 10.4, 3.3 Hz), 4.86–4.91 (1H, m), 6.08 (1H, d, *J* = 15.8 Hz), 6.66 (1H, d, *J* = 8.4 Hz), 6.90 (1H, d, *J* = 1.8 Hz), 6.94 (1H, dd, *J* = 8.5, 2.2 Hz), 6.97–7.01 (2H, m), 7.34 (1H, d, *J* = 8.4 Hz), 7.37 (1H, d, *J* = 16.4 Hz). ¹³C NMR (CDCl₃) δ: 177.4, 154.0, 150.2, 140.9, 135.6, 135.1, 130.7, 130.7, 130.2, 126.2, 126.1, 125.7, 125.3, 123.8, 121.0, 116.3, 110.0, 78.0, 69.3, 67.0, 49.0, 29.0, 28.3, 24.0, 20.0, 16.6, 8.3. MS (ESI positive): 581 (M+Na)⁺.

5.1.10. (S)-5-(4-{1-Ethyl-1-[3-methyl-4-(4,4,4-trifluoro-3-hydroxy-3-trifluoromethylbutyl)phenyl]propyl}-2-methylphenoxy)methyl) dihydrofuran-2-one (18)

To a solution of **16** (55 mg, 0.099 mmol) in AcOEt (5 mL) was added Pd(OH)₂/C (20 wt%, 14 mg, 0.020 mmol) and the mixture was stirred at room temperature under H₂ atmosphere overnight. The mixture was filtered through a celite pad and concentrated. The obtained residue was purified by preparative TLC (*n*-hexane/AcOEt = 2:1) to afford **18** (52.5 mg, 95%) as colorless oil. [α_D^{25}] +12.0 (*c* 1.05, CHCl₃). ¹H NMR (CDCl₃) δ: 0.59 (6H, t, *J* = 7.3 Hz), 2.04 (4H, q, *J* = 7.3 Hz), 2.11–2.17 (5H, m), 2.24 (3H, s),

2.30–2.35 (1H, m), 2.38–2.48 (1H, m), 2.52–2.61 (1H, m), 2.73–2.83 (3H, m), 4.05 (1H, dd, *J* = 10.4, 3.5 Hz), 4.16 (1H, dd, *J* = 10.4, 3.3 Hz), 4.86–4.92 (1H, m), 6.66 (1H, d, *J* = 8.4 Hz), 6.91–6.94 (4H, m), 7.00 (1H, d, *J* = 8.6 Hz). ¹³C NMR (CDCl₃) δ: 177.8, 153.9, 147.1, 141.3, 135.2, 134.8, 130.7, 130.1, 127.9, 126.2, 126.0, 125.6, 124.7, 121.8, 109.9, 78.2, 76.1, 69.3, 48.7, 31.0, 29.1, 28.4, 25.2, 24.0, 19.2, 16.6, 8.4. MS (ESI positive): 561 (M+H)⁺.

5.1.11. General procedure for hydrolysis of the lactone group of 16, 17 and 18

To a solution of lactone (0.355 mmol) in methanol (7.5 mL), 1 M KOH solution (0.7 mL, 0.700 mmol) was added. The mixture was stirred at room temperature for 2 h. The mixture was poured into satd NH₄Cl aq solution and products were extracted with AcOEt. The extracts were washed with brine, dried over MgSO₄, and concentrated. The obtained residue was chromatographed on silica gel (5% MeOH/CH₂Cl₂) to afford gamma hydroxycarboxylic acid. Then, the free form of carboxylic acid was diluted in EtOH, 1.0 equiv of 1 M NaOH solution was added and then concentrated. The obtained salt was stored at –30 °C as 1 mg/mL EtOH solution.

5.1.12. (S)-5-(4-{1-Ethyl-1-[3-methyl-4-(4,4,4-trifluoro-3-hydroxy-3-trifluoromethyl-1-butynyl)phenyl]propyl}-2-methylphenoxy)-4-hydroxypentanoic acid sodium salt (5)

The yield was 52%. Colorless amorphous. [α_D^{25}] +2.53 (*c* 0.40, CHCl₃). ¹H NMR (CD₃OD) δ: 0.60 (6H, t, *J* = 7.3 Hz), 1.80–1.87 (1H, m), 1.95–2.03 (1H, m), 2.09 (4H, q, *J* = 7.3 Hz), 2.15 (3H, s), 2.36 (3H, s), 2.39–2.47 (2H, m), 3.90 (2H, d, *J* = 5.1 Hz), 3.95–3.98 (1H, m), 6.77 (1H, d, *J* = 8.6 Hz), 6.85 (1H, d, *J* = 1.8 Hz), 6.94 (1H, dd, *J* = 8.6, 2.5 Hz), 7.03 (1H, dd, *J* = 8.0, 1.6 Hz), 7.09 (1H, s), 7.34 (1H, d, *J* = 8.0 Hz). ¹³C NMR (CD₃OD) δ: 183.2, 157.3, 154.3, 142.6, 141.9, 133.5, 132.3, 131.5, 128.1, 128.0, 127.8, 125.5, 122.7, 118.9, 112.3, 90.1, 83.0, 74.1, 71.7, 51.3, 49.4, 34.5, 31.7, 30.8, 21.5, 17.6, 9.6. HRMS (ESI negative): Calcd for C₂₉H₃₁F₆O₅ 573.2081. Found: 573.2077 (M–H)[–].

5.1.13. (S)-5-(4-{1-Ethyl-1-[3-methyl-4-((E)-4,4,4-trifluoro-3-hydroxy-3-trifluoromethyl-1-butenyl)phenyl]propyl}-2-methylphenoxy)-4-hydroxypentanoic acid sodium salt (6)

The yield was 49%. Colorless amorphous. [α_D^{25}] +2.25 (*c* 0.62, CHCl₃). ¹H NMR (CD₃OD) δ: 0.59 (6H, t, *J* = 7.2 Hz), 1.78–1.88 (1H, m), 1.92–2.00 (1H, m), 2.07 (4H, q, *J* = 7.4 Hz), 2.14 (3H, s), 2.31 (3H, s), 2.33–2.39 (2H, m), 3.89 (2H, d, *J* = 5.1 Hz), 3.92–3.98 (1H, m), 6.16 (1H, d, *J* = 15.8 Hz), 6.77 (1H, d, *J* = 8.6 Hz), 6.84 (1H, d, *J* = 2.0 Hz), 6.93–7.01 (3H, m), 7.33 (1H, d, *J* = 8.0 Hz), 7.40 (1H, d, *J* = 15.8 Hz). ¹³C NMR (CD₃OD) δ: 183.5, 157.2, 152.2, 142.3, 137.4, 136.5, 133.7, 132.4, 132.2, 128.1, 128.1, 127.9, 127.1, 124.3, 121.3, 112.2, 74.1, 72.3, 59.2, 49.8, 36.4, 32.4, 30.9, 21.0, 17.6, 9.6. HRMS (ESI negative): Calcd for C₂₉H₃₃F₆O₅ 575.2238. Found: 575.2224 (M–H)[–].

5.1.14. (S)-5-(4-{1-Ethyl-1-[3-methyl-4-(4,4,4-trifluoro-3-hydroxy-3-trifluoromethylbutyl)phenyl]propyl}-2-methylphenoxy)-4-hydroxypentanoic acid sodium salt (7)

The yield was 83%. Colorless amorphous. [α_D^{25}] +1.38 (*c* 0.86, CHCl₃). ¹H NMR (CD₃OD) δ: 0.58 (6H, t, *J* = 7.3 Hz), 1.77–1.87 (2H, m), 1.95–2.02 (2H, m), 2.06 (4H, q, *J* = 7.1 Hz), 2.15 (3H, s), 2.23 (3H, s), 2.41–2.55 (2H, m), 2.76–2.81 (2H, m), 3.89 (2H, dd, *J* = 5.1, 1.2 Hz), 3.94–4.00 (1H, m), 6.73 (1H, d, *J* = 8.3 Hz), 6.87 (1H, d, *J* = 2.0 Hz), 6.92–6.96 (3H, m), 6.99 (1H, d, *J* = 8.8 Hz). ¹³C NMR (CD₃OD) δ: 178.0, 155.9, 148.3, 141.6, 136.8, 135.6, 131.3, 131.0, 128.8, 127.1, 126.9, 126.6, 126.3, 123.5, 111.2, 73.0, 70.2, 68.6, 49.6, 33.0, 30.5, 30.0, 29.9, 26.2, 19.1, 16.4, 8.5. HRMS (ESI negative): Calcd for C₂₉H₃₅F₆O₅ 577.2394. Found: 575.2389 (M–H)[–].

5.2. VDRE reporter gene assay

MG-63 cells were plated at 2×10^3 cells/200 μ L/well in a 96-well white cell-culture plate and were incubated at 37 °C in 5% CO₂ incubator for 24 h. Then, MG-63 cells were cotransfected with 0.05 μ g of the pGV2-basic/VDRE-luciferase vector which contained three repeats of the VDRE sequence from mouse osteopontin promoter and 0.001 μ g of pRL-SV40 vector (Promega Corporation, WI, USA) using Lipofectamine (Invitrogen). The cells were added to minimum essential medium (MEM) containing 5% fetal bovine serum treated with dextran-coated charcoal (DCC-FBS) and were incubated for 8 h. The cells were treated with the serial diluted compounds (final concentrations were 10^{-7} to 10^{-11} mol/L with 0.1% DMSO) and were incubated for an additional 3 days. After removing the supernatants, the cells were lysed in cell-lysis buffer and luciferase activity was measured by DLR™ Assay System (Promega Corporation, WI, USA) and the luminescence was detected by Wallac ALVO SX 1420 multi-label counter (PerkinElmer, Inc., MA, USA). The half maximal effective concentrations (EC₅₀) were determined and the inductive activity was calculated as the ratio of the EC₅₀ value of the compounds to that of 1,25(OH)₂D₃ (Solvay Pharmaceuticals, Weesp, The Netherlands), which was used as a positive control.

5.3. Osteocalcin induction assay

MG-63 cells were plated at 2×10^3 cells/well in 200 μ L of serum-free MEM in a 96-well plate and were incubated at 37 °C in 5% CO₂ for 24 h. After washing cells with 5% DCC-FBS/MEM (culture medium), the cells were added to culture medium and treated with the serial diluted compounds (final concentrations were 10^{-7} to 10^{-11} mol/L with 0.1% DMSO), and incubated for 8 h. After changing the culture medium to a fresh one, the cells were incubated for an additional 4 days, and then supernatant was collected and stored at –80 °C.

The frozen supernatant was thawed slowly at room temperature and Gla-type osteocalcin EIA kit (Takara Bio. Inc, Tokyo, Japan) was used to measure osteocalcin. Absorbance at 450 nm was measured on a plate reader (Model 3550, Bio-Rad Laboratories, CA, USA) and each concentration was calculated by comparison with standards using μ plate Manager III software (Bio-Rad Laboratories). The EC₅₀ value was determined and the inductive activity was calculated as the ratio of the EC₅₀ value of the compounds to that of 1,25(OH)₂D₃.

5.4. HL-60 cell differentiation assay

Human promyelocytic leukemic HL-60 cells (2×10^5 cells/mL) in a 96-well micro-titer plate were seeded in 100 μ L of PRMI-1640 medium with antibiotics and 10% heat-inactivated fetal bovine serum at 37 °C in a humidified atmosphere of 5% CO₂ in air. To examine the effects of the analogs on cell differentiation, HL-60 cells were cultured for 4 days with or without different concentrations (10^{-10} to 10^{-7} M) of analogs. On the last day of incubation, 20 μ L of detection mixture reagent consisting of PMA (final 100 ng/mL) and WST-8 reagent (final 20%), was added and incubated for an additional 90 minutes in the same conditions. After incubation, the change of absorbance at 450 nm was measured with the plate reader. The EC₅₀ value was determined and the cell differentiation activity was calculated as the ratio of the EC₅₀ value of the compounds to that of 1,25(OH)₂D₃.

5.5. Crystallographic structure analysis

Protein sample preparation and crystallization were based on the methods by Moras et al.^{42,43} X-ray diffraction data collection

Table 3

Crystal and diffraction data of VDR with compounds **6** and **5**

	6	5
Wavelength (Å)	1.0	1.0
Cell (Å)		
<i>a</i>	44.4	44.6
<i>b</i>	51.9	51.8
<i>c</i>	132.1	132.5
Resolution (Å)	1.9	1.8
Completeness (last shell) (%)	93.5 (89.3)	91.3 (72.1)
<i>R</i> _{sym} (last shell) (%)	12.2 (35.8)	6.2 (15.7)
<i>I</i> / σ (last shell)	4.0 (2.0)	6.4 (4.3)
<i>R</i> _{cryst}	20.1	19.4
Rmsd bond length (Å)	0.010	0.010
Rmsd bond angles (deg)	0.98	0.94
No. of non-hydrogen protein atoms	1993	1993
No. of water molecules	195	266

and data processing were carried out by generally accepted methods. After brief soaking in the buffer containing 30% glycerol, 0.6 M ammonium sulfate and 0.1 M MES (pH 6.0), crystals were trapped in the fiber loops and flash-cooled with liquid nitrogen. Crystals were stored and transported in a dry shipper. Data collections were carried out at the synchrotron beamline BL32B2 of the Spring-8 facility in Hyogo, Japan, operated by the Pharmaceutical Consortium for Protein Structure Analysis. Crystals were kept frozen during data collection with a vapor stream of liquid nitrogen. X-ray diffraction data was collected with the R-Axis V imaging plate area detector. The crystals were isomorphous with the space group P212121 reported by Moras et al.^{42,43} for the 1,25(OH)₂D₃-VDR complex. Data were processed with CCP4 and MOSFLM. The initial structure model for the refinement was constructed by removing all the water and the ligand atoms in the 1,25(OH)₂D₃-VDR complex structure in the Protein Databank (PDB ID: 1db1). A rigid body refinement was followed by simulated annealing using the CNX. Electron density in the ligand-binding pocket clearly and unambiguously showed the ligand conformation. After fitting the ligand model into the electron density, structure refinement was continued with the software autoBUSTER and the water molecules were placed automatically. The data collection and the refinement statistics are summarized in Table 3.

5.6. Modeling and volume calculations

The compounds **5**, **6**, and **7** were manually docked in the crystal structure of the VDR (PDB ID: 3AZ3). The conformations of compounds were optimized using the MAB force field as implemented in the program MOLOC⁴⁴ with the VDR structure fixed. Based on the docking structures of the VDR with **5**, **6**, and **7**, the PC values (the volume occupied by the side chain of the compound) of compounds **5**, **6**, and **7** were calculated as described in Ref. 32.

Acknowledgements

The authors thank Ms. Hitomi Suda of Chugai Pharmaceutical Co., Ltd for HRMS measurements of the compounds and Editing Services of Chugai Pharmaceutical Co., Ltd for proofreading the manuscript.

References and notes

- Muller, K.; Faeh, C.; Diederich, F. *Science* **1881**, 2007, 317.
- Paulini, R.; Muller, K.; Diederich, F. *Angew. Chem., Int. Ed.* **2005**, *44*, 1788.
- Zhou, P.; Zou, J.; Tian, F.; Shang, Z. *J. Chem. Inf. Model.* **2009**, *49*, 2344.
- Iwaoka, M.; Komatsu, H.; Katsuda, T.; Tomoda, S. *J. Am. Chem. Soc.* **1902**, 2002, 124.
- Matta, C. F.; Castillo, N.; Boyd, R. *J. Phys. Chem. A* **2005**, *109*, 3669.
- Lee, S.; Mallik, A. B.; Fredrickson, D. C. *Cryst. Growth Des.* **2004**, *4*, 279.

7. Olsen, J. A.; Banner, D. W.; Seiler, P.; Sander, U. O.; D'Arcy, A.; Stihle, M.; Mueller, K.; Diederich, F. *Angew. Chem., Int. Ed.* **2003**, *42*, 2507.
8. Plenio, H. *ChemBioChem* **2004**, *5*, 650.
9. Bettinger, H. F. *ChemPhysChem* **2005**, *6*, 1169.
10. Lu, Y.; Zou, J.; Yu, Q.; Jiang, Y.; Zhao, W. *Chem. Phys. Lett.* **2007**, *449*, 6.
11. Awwadi, F. F.; Willett, R. D.; Peterson, K. A.; Twamley, B. *J. Phys. Chem. A* **2007**, *111*, 2319.
12. Awwadi, F. F.; Willett, R. D.; Peterson, K. A.; Twamley, B. *Chem. -Eur. J.* **2006**, *12*, 8952.
13. Kawahara, S.; Tsuzuki, S.; Uchimaru, T. *J. Phys. Chem. A* **2004**, *108*, 6744.
14. Riley, K. E.; Merz, K. M., Jr. *J. Phys. Chem. B* **2005**, *109*, 17752.
15. Chopra, D.; Nagarajan, K.; Row, T. N. G. *J. Mol. Struct.* **2008**, *888*, 70.
16. Tanaka, Y.; DeLuca, H. F.; Schnoes, H. K.; Ikekawa, N.; Kobayashi, Y. *Arch. Biochem. Biophys.* **1980**, *199*, 473.
17. Kobayashi, Y.; Taguchi, T.; Mitsuhashi, S.; Eguchi, T.; Ohshima, E.; Ikekawa, N. *Chem. Pharm. Bull.* **1982**, *30*, 4297.
18. Tanaka, Y.; DeLuca, H. F.; Kobayashi, Y.; Ikekawa, N. *Arch. Biochem. Biophys.* **1984**, *229*, 348.
19. Inaba, M.; Okuno, S.; Nishizawa, Y.; Yukioka, K.; Otani, S.; Matsui-Yuasa, I.; Morisawa, S.; DeLuca, H. F.; Morii, H. *Arch. Biochem. Biophys.* **1987**, *258*, 421.
20. Inaba, M.; Okuno, S.; Nishizawa, Y.; Imanishi, Y.; Katsumata, T.; Sugata, I.; Morii, H. *Biochem. Pharmacol.* **1993**, *45*, 2331.
21. Sheves, M.; Sialom, B.; Mazur, Y. J. C. S. *Chem. Commun.* **1978**, *13*, 554.
22. Napoli, J. L.; Fivizzani, M. A.; Schnoes, H. K.; DeLuca, H. F. *Biochemistry* **1978**, *17*, 2387.
23. Ohshima, E.; Sai, H.; Takatsuto, S.; Ikekawa, N.; Kobayashi, Y.; Tanaka, Y.; DeLuca, H. F. *Chem. Pharm. Bull.* **1984**, *32*, 3525.
24. Boehm, M. F.; Fitzgerald, P.; Zou, A.; Elgort, M. G.; Bischoff, E. D.; Mere, L.; Mais, D. E.; Bissonnette, R. P.; Heyman, R. A.; Nadzan, A. M.; Reichman, M.; Allegretto, E. A. *Chem. Biol.* **1999**, *6*, 265.
25. Swann, S. L.; Bergh, J.; Farach-Carson, M. C.; Ocasio, C. A.; Koh, J. T. *J. Am. Chem. Soc.* **2002**, *124*, 13795–13805.
26. Peräkylä, M.; Malinen, M.; Herzig, K. H.; Carlberg, C. *Mol. Endocrinol.* **2005**, *19*, 2060–2073.
27. Hosoda, S.; Tanatani, A.; Wakabayashi, K.; Nakano, Y.; Miyachi, H.; Nagasawa, K.; Hashimoto, Y. *Bioorg. Med. Chem. Lett.* **2005**, *15*, 4327–4331.
28. Ma, Y.; Khalifa, B.; Yee, Y. K.; Lu, J.; Memezawa, A.; Savkur, R. S.; Yamamoto, Y.; Chintalacheruvu, S. R.; Yamaoka, K.; Stayrook, K. R.; Bramlett, K. S.; Zeng, Q. Q.; Chandrasekhar, S.; Yu, X. P.; Linebarger, J. H.; Iturria, S. J.; Burris, T. P.; Kato, S.; Chin, W. W.; Nagpal, S. *J. Clin. Invest.* **2006**, *116*, 892–904.
29. Hosoda, S.; Tanatani, A.; Wakabayashi, K.; Makishima, M.; Imai, K.; Miyachi, H.; Nagasawa, K.; Hashimoto, Y. *Bioorg. Med. Chem.* **2006**, *14*, 5489–5502.
30. Demizu, Y.; Takahashi, T.; Kaneko, F.; Sato, Y.; Okuda, Y.; Ochiai, E.; Horie, K.; Takagi, K.; Kakuda, S.; Takimoto-Kamimura, M.; Kurihara, M. *Bioorg. Med. Chem. Lett.* **2011**, *21*, 6104–6107.
31. Kashiwagi, H.; Ono, Y.; Shimizu, K.; Haneishi, T.; Ito, S.; Iijima, S.; Kobayashi, T.; Ichikawa, F.; Harada, S.; Sato, H.; Sekiguchi, N.; Ishigai, M.; Takahashi, T. *Bioorg. Med. Chem.* **2011**, *19*, 4721.
32. Kashiwagi, H.; Ono, Y.; Ohta, M.; Morikami, K.; Takahashi, T. *Bioorg. Med. Chem.* **2012**, *20*, 4495.
33. Brown, J. P.; Malaval, L.; Chapuy, M. C.; Delmas, P. D.; Edouard, C.; Meunier, J. *Lancet* **1984**, *323*, 1091.
34. Lian, J. B.; Stein, J. L.; Stein, G. S.; Montecino, M.; van Wijnen, A. J.; Javed, A.; Gutierrez, S. *Steroids* **2001**, *66*, 159.
35. Paredes, R.; Arriagada, G.; Cruzat, F.; Olate, J.; van Wijnen, A.; Lian, J.; Stein, G.; Stein, J.; Montecino, M. *J. Steroid Biochem. Mol. Biol.* **2004**, *89–90*, 269.
36. Milletti, F.; Storch, L.; Sforza, G.; Cruciani, G. *J. Chem. Inf. Model.* **2007**, *47*, 2172.
37. Svensson, S.; Östberg, T.; Jacobsson, M.; Norström, C.; Stefansson, K.; Hallén, D.; Johansson, I. C.; Zachrisson, K.; Ogg, D.; Jendeberg, L. *EMBO J.* **2003**, *22*, 4625.
38. Eelen, G.; Valle, N.; Sato, Y.; Rochel, N.; Verlinden, L.; De Clercq, P.; Moras, D.; Bouillon, R.; Muñoz, A.; Verstuyf, A. *Chem. Biol.* **2008**, *15*, 1029.
39. Huet, T.; Maehr, H.; Lee, H. J.; Uskokovic, M. R.; Suh, N.; Moras, D.; Rochel, N. *Med. Chem. Commun.* **2011**, *2*, 424.
40. Daylight Chemical Information Systems, Inc.; Laguna Niguel, CA 92677, USA.
41. Toyota, S. *Chem. Rev.* **2010**, *110*, 5398.
42. Juntunen, K.; Rochel, N.; Moras, D.; Vihko, P. *Biochem. J.* **1999**, *344*, 297.
43. Rochel, N.; Wurtz, J. M.; Mitschler, A.; Klaholz, B.; Moras, D. *Mol. Cell* **2000**, *5*, 173.
44. Gerber, P. R.; Müller, K. *J. Comput. Aided Mol. Des.* **1995**, *9*, 251.